Gooley, P. R., Blunt, J. W., Beress, L., & Norton, R. S. (1988) *Biopolymers 27*, 1143–1157.
Imoto, T., Johnson, L. N., North, A. C. T., Phillips, D. C., & Rupley, J. A. (1972) *Enzymes (3rd Ed.) 7*, 665–868.
Kaptein, R. (1982) in *Biological Magnetic Resonance* (Berliner, L., & Reuben, J., Eds.) Vol. 4, pp 145–191, Plenum Press, New York.
Kem, W. R. (1988) in *The Biology of Nematocysts* (Hessinger, D., & Lenhoff, H., Eds.) pp 375–405, Academic Press, New York.
Kem, W. R., Dunn, B. M., Parten, B. F., Pennington, M. W., & Price, D. (1986) *Fed. Proc., Fed. Am. Soc. Exp. Biol. 45*, 1795.
Metrione, R. M., Schweitz, H., & Walsh, K. A. (1987) *FEBS Lett. 218*, 59–62.
Norton, R. S., & Norton, T. R. (1979) *J. Biol. Chem. 254*, 10220–10226.
Norton, R. S., Zwick, J., & Beress, L. (1980) *Eur. J. Biochem. 113*, 75–83.
Norton, R. S., Norton, T. R., Sleigh, R. W., & Bishop, D. G. (1982) *Arch. Biochem. Biophys. 213*, 87–97.
Norton, R. S., Beress, L., Stob, S., Boelens, R., & Kaptein, R. (1986) *Eur. J. Biochem. 157*, 343–346.
Norton, T. R. (1981) *Fed. Proc., Fed. Am. Soc. Exp. Biol. 40*, 21–25.
Pennington, M. W., Kem, W. R., & Dunn, B. M. (1988) in *Macromolecular Sequencing and Analysis. Selected Methods and Applications* (Schlesinger, D. H., Ed.) pp 243–250, Liss, New York.
Schweitz, H., Vincent, J.-P., Barhanin, J., Frelin, C., Linden, G., Hugues, M., & Lazdunski, M. (1981) *Biochemistry 20*, 5245–5252.
Schweitz, H., Bidard, J.-N., Frelin, C., Pauron, D., Vijverberg, H. P. M., Mahasneh, D. M., Lazdunski, M., Vilbois, F., & Tsugita, M. (1985) *Biochemistry 24*, 3554–3561.
Torda, A. E., & Norton, R. S. (1987) *Biochem. Int. 15*, 659–666.
Torda, A. E., Mabbutt, B. C., van Gunsteren, W. F., & Norton, R. S. (1988) *FEBS Lett.* (in press).
Wagner, G., & Wüthrich, K. (1978) *Nature 275*, 247–248.
Wemmer, D. E., Kumar, N. V., Metrione, R. M., Lazdunski, M., Drobny, G., & Kallenbach, N. R. (1986) *Biochemistry 25*, 6842–6849.
Widmer, H., Wagner, G., Schweitz, H., Lazdunski, M., & Wüthrich, K. (1988) *Eur. J. Biochem. 171*, 177–192.
Wüthrich, K. (1986) *NMR of Proteins and Nucleic Acids*, Wiley, New York.
Zykova, T. A., Vinokurov, L. M., Kozlovskaya, E. P., & Elyakov, G. B. (1985) *Bioorg. Khim. 11*, 302–310.

Sequence-Specific ^{1}H NMR Assignments and Secondary Structure in the Sea Anemone Polypeptide *Stichodactyla helianthus* Neurotoxin I†

Rasmus H. Fogh,‡ Bridget C. Mabbutt,‡ William R. Kem,§ and Raymond S. Norton*,‡
School of Biochemistry, University of New South Wales, Kensington, New South Wales 2033, Australia, and Department of Pharmacology and Therapeutics, University of Florida, Gainesville, Florida 32610
Received August 3, 1988; Revised Manuscript Received September 21, 1988

ABSTRACT: Sequence-specific assignments are reported for the 500-MHz ^{1}H nuclear magnetic resonance (NMR) spectrum of the 48-residue polypeptide neurotoxin I from the sea anemone *Stichodactyla helianthus* (Sh I). Spin systems were first identified by using two-dimensional relayed or multiple quantum filtered correlation spectroscopy, double quantum spectroscopy, and spin lock experiments. Specific resonance assignments were then obtained from nuclear Overhauser enhancement (NOE) connectivities between protons from residues adjacent in the amino acid sequence. Of a total of 265 potentially observable resonances, 248 (i.e., 94%) were assigned, arising from 39 completely and 9 partially assigned amino acid spin systems. The secondary structure of Sh I was defined on the basis of the pattern of sequential NOE connectivities, NOEs between protons on separate strands of the polypeptide backbone, and backbone amide exchange rates. Sh I contains a four-stranded antiparallel β-sheet encompassing residues 1–5, 16–24, 30–33, and 40–46, with a β-bulge at residues 17 and 18 and a reverse turn, probably a type II β-turn, involving residues 27–30. No evidence of α-helical structure was found.

In the preceding paper (Norton et al., 1989) we presented the results of an investigation by ^{1}H NMR spectroscopy of the solution properties of the polypeptide neurotoxin I (Sh I)[1] from the Caribbean sea anemone *Stichodactyla helianthus*. This molecule is a representative of a new class of sea anemone polypeptides that are neurotoxic by virtue of their specific interaction with the nerve sodium channel (Kem, 1988). Other members of this class are *Heteractis* [formerly *Radianthus* (Dunn, 1981)] *macrodactylus* toxin III (Zykova et al., 1985)

† This work was supported in part by grants from the Australian Research Grants Scheme (R.S.N.) and the National Institutes of Health (Grant GM 32848 to W.R.K.). One of us (R.H.F.) thanks the Danish Medical Research Council and the Carlsberg Foundation for travel grants.
* Address correspondence to this author.
‡ University of New South Wales.
§ University of Florida.

[1] Abbreviations: Sh I, *Stichodactyla* (formerly *Stoichactis*) *helianthus* neurotoxin I; Hm III, *Heteractis* (formerly *Radianthus*) *macrodactylus* toxin III; Hp II and III, *Heteractis* (formerly *Radianthus*) *paumotensis* toxins II and III; AP-A, anthopleurin A; ATX I and II, *Anemonia sulcata* toxins I and II; 2D, two dimensional; DQF- (or TQF-) COSY, double (or triple) quantum filtered 2D homonuclear correlated spectroscopy; NOESY, 2D homonuclear nuclear Overhauser enhancement spectroscopy; RELAY, 2D homonuclear relayed coherence transfer spectroscopy; DQ, 2D homonuclear double quantum coherence spectroscopy; HOHAHA, 2D homonuclear Hartmann–Hahn spectroscopy; NOE, nuclear Overhauser enhancement; $d_{AB}(i,j)$, distance between proton type A and B located, respectively, in amino acid residues i and j; d_{AB}, the sequential connectivity $d_{AB}(i,i+1)$.

0006-2960/89/0428-1826$01.50/0

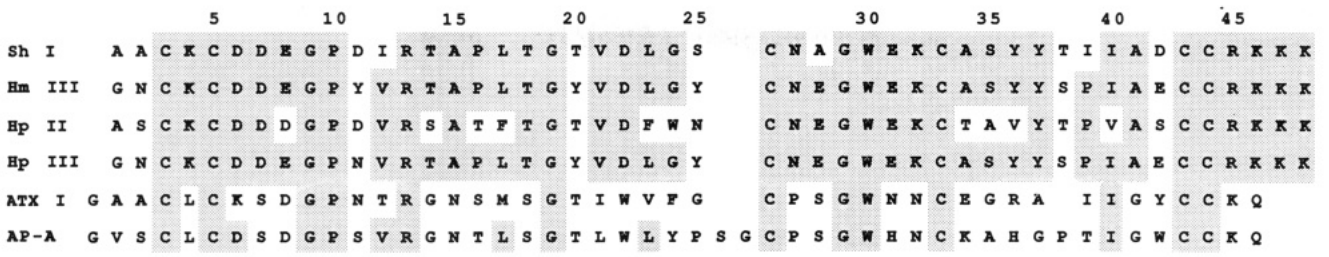

FIGURE 1: Amino acid sequences of Sh I (Kem et al., 1986), Hm III (Zykova et al., 1985), Hp II (Wemmer et al., 1986), Hp III (Metrione et al., 1987), ATX I (Beress, 1982), and AP-A (Norton, 1981). Shaded boxes indicate conserved residues.

and *Heteractis paumotensis* toxins II (Schweitz et al., 1985; Wemmer et al., 1986) and III (Metrione et al., 1987), as shown in Figure 1.

These neurotoxins are similar in many respects to polypeptides from anemones of the family Actiniidae, typified by AP-A from *Anthopleura xanthogrammica* (Norton, 1981) and ATX I and II from *Anemonia sulcata* (Beress, 1982). However, a number of significant differences between the two classes of polypeptide have been noted, involving their sequences at the N- and C-termini (Figure 1), the distribution of charged residues (Kem, 1988), their mode of binding to the sodium channel, and their immunological cross-reactivity (Schweitz et al., 1985). In the preceding paper (Norton et al., 1989) we found that these differences also extend to the solution properties of these polypeptides. The pH dependence of Sh I, the specific ionic interactions that stabilize its tertiary structure, and its thermal stability all differ from those of AP-A and ATX I and II (Gooley et al., 1988).

In order to interpret the various differences between the two classes of polypeptides, it is necessary to determine their three-dimensional structures in solution. To this end we have undertaken a ^{1}H NMR study of the solution structure of Sh I, which can then be compared with our recently determined structure of AP-A (Torda et al., 1988). In this paper we present sequence-specific ^{1}H resonance assignments for Sh I. These data also provide a description of the ordered secondary structure of Sh I, which is compared with those for AP-A (Gooley & Norton, 1986), ATX I (Widmer et al., 1988), and Hp II (Wemmer et al., 1986).

Materials and Methods

Sh I was isolated from the sea anemone *Stichodactyla helianthus* collected in the Caribbean, as described by Kem et al. (1986). High-performance liquid chromatography of the purified material on a Vydac-C18 column (Gooley et al., 1988) showed that it contained minor polypeptide components comprising up to 10–15% of the material. These additional components were evident in the NMR spectra but did not cause problems in the data analysis. Other materials were as described in the preceding paper (Norton et al., 1989). Samples for 2D NMR contained 6–9 mM Sh I in either H_2O or 90% H_2O/10% D_2O at pH values in the range 3.0–6.5. The pH values quoted are uncorrected meter readings at room temperature.

All NMR spectra were recorded and processed on a Bruker AM 500 spectrometer equipped with an ASPECT 3000 computer with process controller. Except as otherwise noted, all experiments were carried out at 27 °C. In all experiments the carrier was set in the center of the spectrum, and quadrature detection was used in both dimensions. All two-dimensional (2D) spectra were recorded in phase-sensitive mode by using the time-proportional phase incrementation (TPPI) method (Marion & Wüthrich, 1983). NOESY spectra (Jeener et al., 1979; Macura et al., 1981) were recorded in D_2O with a mixing time of 120 ms and in H_2O with mixing times of 180 ms (at 12 °C), 230 ms, and 250 ms. DQF-COSY experiments (Piantini et al., 1982; Shaka & Freeman, 1983) were acquired by using $90°_x90°_y$ composite 90° pulses according to Müller et al. (1986). A TQF-COSY experiment was recorded according to Piantini et al. (1982). HOHAHA spin lock experiments using the MLEV-17 sequence (Braunschweiler & Ernst, 1983; Bax & Davis, 1985) were recorded with mixing times ranging from 32 to 65 ms. In order to detect slowly exchanging backbone amide protons, one HOHAHA experiment was carried out at 12 °C on a fully protonated Sh I sample immediately after dissolution in D_2O. A RELAY experiment (Wagner, 1983; Bax & Drobny, 1985) and a double quantum (DQ) experiment (Wokaun & Ernst, 1977; Wagner & Zuiderweg, 1983) were performed on a sample in H_2O. A total mixing time of 40 ms was used for the RELAY and a preparation time of 50 ms was employed for the DQ experiment. The $90°_x180°_y90°_x$ composite 180° pulse (Levitt & Freman, 1979) was used for refocusing in both experiments.

Solvent suppression was carried out by using presaturation during the relaxation delay. For HOHAHA experiments the solvent irradiation was switched off during the t_1 evolution period. In all other experiments the sample was irradiated during preparation, t_1, and mixing times at a decoupler power setting 5–10 dB lower than for presaturation. The relaxation delay was typically 1.8 s, but values from 1.4 to 2.0 s were used. Spectral widths were 6024 Hz in H_2O and 5000 Hz in D_2O, acquired over 4K data points. HOHAHA experiments were recorded over 12–18 h, with 216–512 t_1 increments and 40–120 scans per increment. Other experiments were recorded over 36–46 h, typically with 512 t_1 increments and 96 scans per increment. Data were zero-filled to 2K in ω_1 and 8K in ω_2, giving a digital resolution of 4.9–5.9 Hz in ω_1 and 1.2–1.5 Hz in ω_2. Before Fourier transformation, phase-shifted sine-squared window functions were applied, with shifts typically being 45°–60° in ω_1 and 30°–45° in ω_2. Spectra are presented as contour plots with no distinction between positive and negative peaks and with successive plotting levels differing by a factor of 2.

Results

Assignment of the proton NMR spectrum of Sh I essentially followed the three-step procedure outlined by Billeter et al. (1982). First, the resonances from nonlabile protons in each amino acid spin system were identified by using experiments carried out in D_2O solution. Experiments in H_2O solution were then used to assign backbone NH protons. Finally, the spin systems were combined into segments by using the sequential NOE connectivities $d_{\alpha N}$, d_{NN}, and $d_{\beta N}$, and the position of these segments was determined by matching them with the known primary structure of the protein. Once the assignments were completed, the secondary structure of the protein was established from the connectivity patterns characteristic of the different secondary structure types.

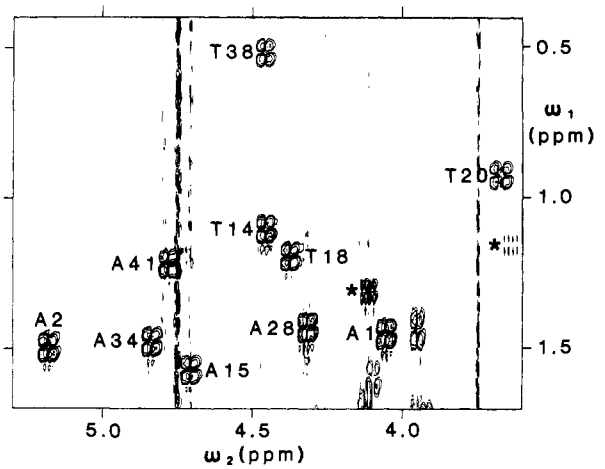

FIGURE 2: CH–CH_3 region of a DQF-COSY spectrum of Sh I at pH 5.0, 27 °C. $C^{\alpha}H$–$C^{\beta}H_3$ peaks of Ala and $C^{\beta}H$–$C^{\gamma}H_3$ peaks of Thr are marked. The two cross-peaks marked with an asterisk (*) are from impurities.

Assignment of Spin Systems. For the purpose of assignment the amino acids are conveniently grouped as follows: Gly; Ala and Thr; Leu, Ile, and Val; long-chain spin systems (Glu, Gln, Met, Pro, Arg, Lys); and AMX spin systems (Phe, Tyr, Trp, His, Cys, Asp, Asn, Ser). The assignments for Sh I are shown in Table I. All four glycine spin systems were identified by starting with the NH–($C^{\alpha}H$+$C^{\alpha}H$) remote peaks in the DQ spectrum (Braunschweiler et al., 1983). The corresponding $C^{\alpha}H$–$C^{\alpha}H$ cross-peaks in the DQF-COSY could then easily be identified. The six alanine and four threonine spin systems all gave rise to characteristically intense CH–CH_3 cross-peaks in the appropriate region (shown in Figure 2) of the DQF-COSY spectrum (Wüthrich, 1986). Five alanine spin systems showed NH–$C^{\beta}H_3$ RELAY cross-peaks, the sixth being assigned to the N-terminal Ala-1. $C^{\alpha}H$–$C^{\gamma}H_3$ and $C^{\beta}H$–$C^{\gamma}H_3$ cross-peaks were observed for all four threonine spin systems in both NOESY and HOHAHA spectra.

The analysis of HOHAHA experiments in D_2O proved a good starting point for assigning Val, Ile, and Leu resonances, as well as those of the long-chain spin systems. In a HOHAHA spectrum every resonance in a given spin system can in principle show cross-peaks to every other, so it was often possible to obtain all the frequencies in a spin system from a single row or column in the HOHAHA spectrum. Moreover, the large number of cross-peaks meant that the same set of resonance frequencies reappeared in several regions of the spectrum, thus confirming the assignments. In Figure 3, examples are shown for the Ile-12, Val-21, Lys-46, and Lys-47 spin systems. Once the set of frequencies was known, DQF-COSY, TQF-COSY, and DQ spectra were used to assign each resonance to a specific proton in the amino acid residue. The single Val, two Leu, and three Ile spin systems were all assigned in this way. All protons gave rise to cross-peaks in DQF-COSY spectra, but in most cases the two ends of each spin system could be connected only by using HOHAHA data. The $C^{\alpha}H$–$C^{\delta}H_3$ cross-peaks observed for two Ile and both Leu spin systems were particularly useful for this purpose.

The spin systems of Pro-10, Pro-16, Arg-13, Glu-31, Lys-46, Lys-47, and Lys-48 were completely assigned as described above, except for the labile protons in the side chains (see Figure 3 for examples). The near degeneracy of the two methylene resonances from each $C^{\delta}H_2$ group in Lys-46, Lys-47, and Lys-48, as well as the $C^{\beta}H_2$, $C^{\gamma}H_2$, and $C^{\delta}H_2$ groups of Arg-13, was confirmed by remote peaks in the DQ spectrum. Because of extensive peak overlap the spin systems

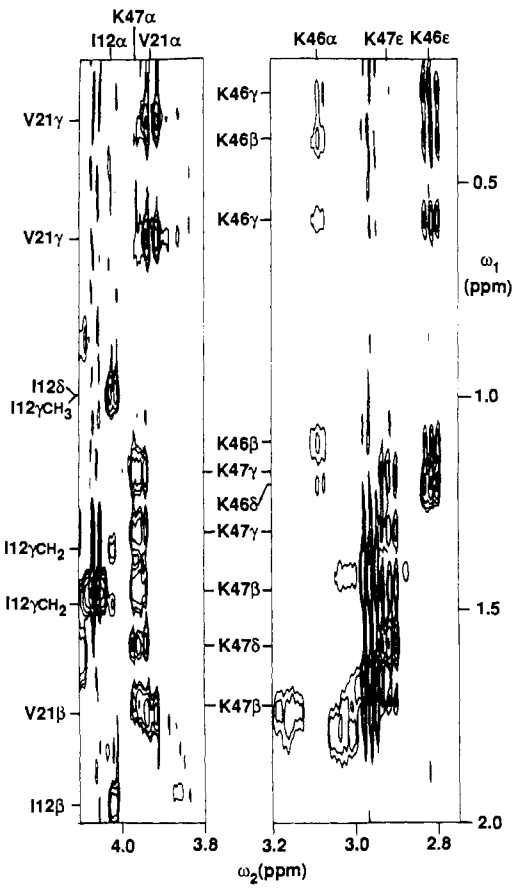

FIGURE 3: HOHAHA spectrum of Sh I in D_2O at pH 5.0 and 27 °C, recorded with 32-ms mixing time. Cross-peaks to Ile-12 $C^{\alpha}H$, Val-21 $C^{\alpha}H$, Lys-46 $C^{\alpha}H$ and $C^{\epsilon}H_2$, and Lys-47 $C^{\alpha}H$ and $C^{\epsilon}H_2$ are marked.

later assigned to Lys-4, Lys-32, and Arg-45 could not be completely assigned initially and were classified only as "long side chain" spin systems. The assignments were completed after the sequential assignment stage when the residue type corresponding to these spin systems was known. The two ends of the spin systems of Lys-32 and Arg-45 were connected by using respectively $C^{\alpha}H$–$C^{\epsilon}H$ and $C^{\alpha}H$–$C^{\delta}H$ cross-peaks in HOHAHA spectra, while the Lys-4 $C^{\delta}H_2$ and $C^{\epsilon}H_2$ resonances were assigned by elimination. In the arginine guanidino groups, $N^{\epsilon}H$ resonances were assigned from cross-peaks to $C^{\gamma}H$ or $C^{\delta}H$ observed in DQ, DQF-COSY, and HOHAHA spectra. In a similar fashion lysine $N^{\zeta}H_3^+$ resonances were identified from HOHAHA cross-peaks to $C^{\delta}H$ and $C^{\epsilon}H$. The side-chain protons of Glu-8 gave rise to no cross-peaks that were not at least partially overlapped, but the spin system was identified from intraresidue NOEs to the backbone NH during sequential assignment. In both Lys-4 and Glu-8, one resonance could not be assigned to a specific proton in the side chain, as it was observed only in HOHAHA experiments.

With two exceptions, assignment of the AMX systems was straightforward. Cross-peaks from Cys-3 were hidden by solvent presaturation or overlap with the diagonal in most spectra. The spin system was assigned by using $C^{\alpha}H$–$C^{\beta}H$ cross-peaks observed in a NOESY experiment in D_2O (Figure 4) and $C^{\beta}H$–$C^{\beta}H$ cross-peaks observed in the DQ experiment. For Ser-35 the $C^{\beta}H$ resonances were degenerate and only one $C^{\alpha}H$–$C^{\beta}H$ cross-peak could be seen. The frequency of the second $C^{\beta}H$ resonance was found from $C^{\alpha}H$–($C^{\beta}H$+$C^{\beta}H$) and $C^{\beta}H$–$C^{\beta}H$ cross-peaks in the DQ spectrum. Both serine spin systems were identified from chemical shifts. Connection of the ring proton resonances of aromatic residues with their

Table I: Chemical Shifts of Assigned Resonances in Sh I in Aqueous Solution at pH 5.0 and 27 °C[a]

residue	NH	$C^{\alpha}H$	$C^{\beta}H$	other
Ala-1	*b*	4.06	1.46	
Ala-2	8.63	5.17	1.51	
Cys-3[c]	7.98	4.71	2.70, 2.81	
Lys-4	8.61	4.47	1.92	$C^{\gamma}H_2$;[d] $C^{\delta}H_2$, 1.81; $C^{\epsilon}H_2$, 2.88, 3.04; $N^{\zeta}H_3^+$, 7.51
Cys-5	9.30	4.55	2.78, 3.23	
Asp-6	8.92	4.42	2.73, 2.88	
Asp-7	8.62	4.38	2.61, 3.04	
Glu-8	7.53	4.23	2.02[e]	$C^{\gamma}H_2$, 2.32[e]
Gly-9	7.75	3.97, 4.44		
Pro-10		4.43	2.05, 2.24	$C^{\gamma}H_2$, 1.98, 2.07; $C^{\delta}H_2$, 3.57, 3.75
Asp-11	8.19	4.78	2.54, 2.93	
Ile-12	8.41	4.02	1.96	$C^{\gamma}H_2$, 1.36, 1.50; $C^{\gamma}H_3$, 1.00; $C^{\delta}H_3$, 0.96
Arg-13	8.43	4.19	1.94, 1.98	$C^{\gamma}H_2$, 1.73, 1.73; $C^{\delta}H_2$, 3.26, 3.26; $N^{\epsilon}H$, 7.57
Thr-14	7.31	4.43	4.47	$C^{\gamma}H_3$, 1.12
Ala-15	7.29	4.71	1.58	
Pro-16		4.33	1.83, 2.25	$C^{\gamma}H_2$, 1.93, 2.06; $C^{\delta}H_2$, 3.87, 4.04
Leu-17	9.06	4.23	0.90, 2.38	$C^{\gamma}H$, 1.59; $C^{\delta}H_3$, 0.74, 0.82
Thr-18	10.47	4.36	4.39	$C^{\gamma}H_3$, 1.21
Gly-19	8.67	3.65, 4.59		
Thr-20	9.90	4.82	3.68	$C^{\gamma}H_3$, 0.95
Val-21	8.03	3.93	1.74	$C^{\gamma}H_3$, 0.37, 0.64
Asp-22	8.85	4.90	2.60, 2.73	
Leu-23	8.35	4.10	1.59, 1.61	$C^{\gamma}H$, 1.65; $C^{\delta}H_3$, 0.85, 0.91
Gly-24	9.01	3.33, 4.33		
Ser-25	8.16	4.61	3.84, 3.92	
Cys-26[c]	8.64	4.77	2.71, 2.96	
Asn-27	7.94	4.46	1.94, 2.71	$N^{\delta}H_2$, 6.87, 6.87
Ala-28	8.49	4.32	1.44	
Gly-29	9.13	3.73, 4.44		
Trp-30	8.83	4.91	2.93, 3.58	N(1)H, 10.44; C(2)H, 7.26; C(4)H, 7.01; C(5)H, 7.25; C(6)H, 7.25; C(7)H, 7.53
Glu-31	9.42	4.91	1.90, 2.05	$C^{\gamma}H_2$, 2.10, 2.25
Lys-32	8.93	4.27	1.76, 1.87	$C^{\gamma}H_2$, 1.42, 1.59; $C^{\delta}H_2$, 1.74, 1.80; $C^{\epsilon}H_2$, 3.03, 3.16; $N^{\zeta}H_3^+$[f]
Cys-33	9.68	5.24	3.01, 3.27	
Ala-34	7.42	4.84	1.49	
Ser-35	9.49	4.10	3.94, 3.99	
Tyr-36	8.13	4.50	2.75, 3.01	C(2,6)H, 7.03; C(3,5)H, 6.66
Tyr-37	8.89	4.69	2.94, 3.26	C(2,6)H, 7.10; C(3,5)H, 6.71
Thr-38	7.67	4.43	4.47	$C^{\gamma}H_3$, 0.55
Ile-39	8.24	4.23	2.02	$C^{\gamma}H_2$, 1.37, 1.64; $C^{\gamma}H_3$, 1.06; $C^{\delta}H_3$, 0.97
Ile-40	7.19	4.62	2.13	$C^{\gamma}H_2$, 1.02, 1.19; $C^{\gamma}H_3$, 0.91; $C^{\delta}H_3$, 0.83
Ala-41	7.60	4.79	1.23	
Asp-42	8.14	5.23	2.05, 2.54	
Cys-43	9.05	4.67	2.19, 2.79	
Cys-44	9.01	5.60	2.93, 2.98	
Arg-45	9.63	5.06	1.81, 1.94	$C^{\gamma}H_2$, 1.80; $C^{\delta}H_2$, 3.17, 3.33; $N^{\epsilon}H$, 6.99
Lys-46	8.17	3.09	0.41, 1.12	$C^{\gamma}H_2$, 0.30, 0.60; $C^{\delta}H_2$, 1.22, 1.22; $C^{\epsilon}H_2$, 2.82, 2.82; $N^{\zeta}H_3^+$, 7.48
Lys-47	8.15	3.96	1.45, 1.72	$C^{\gamma}H_2$, 1.18, 1.32; $C^{\delta}H_2$,1.58, 1.58; $C^{\epsilon}H_2$, 2.92, 2.92; $N^{\zeta}H_3^+$[f]
Lys-48	8.53	4.13	1.71, 1.78	$C^{\gamma}H_2$, 1.39, 1.44; $C^{\delta}H_2$, 1.66, 1.66; $C^{\epsilon}H_2$, 2.97, 2.97; $N^{\zeta}H_3^+$[f]

[a] Chemical shifts in ppm relative to sodium 2,2-dimethyl-2-silapentane-5 sulfonate (DSS). Estimated accuracy 0.02 ppm. For methylene groups two chemical shifts are indicated only where both protons are assigned; a single entry indicates that it was not established whether the two resonances were degenerate. [b] Protons exchange with solvent too quickly to be observed under present conditions. [c] Assignment of $C^{\alpha}H$ and $C^{\beta}H$ to either Cys-3 or Cys-26 is tentative only, as discussed in text. [d] A resonance at 1.42 ppm is tentatively assigned as $C^{\gamma}H$ on the basis of its chemical shift. [e] A resonance at 2.43 ppm could be assigned as either $C^{\beta}H$ or $C^{\gamma}H$. [f] Additional unassigned NH resonances are observed at 7.04 and 7.57 ppm (see text).

corresponding $C^{\beta}H$ resonances was accomplished by using intraresidue NOEs (Billeter et al., 1982). The peak assigned to the Asn-27 side-chain amide protons was well resolved and showed no through-bond connectivities to other frequencies, except for some weak traces close to the diagonal that were ascribed to an impurity. At pH 5.0 and 27 °C in H_2O this resonance had an intensity corresponding to about two protons and showed NOESY cross-peaks only to the $C^{\alpha}H$ and $C^{\beta}H$ resonances of Asn-27. In NOESY experiments at 12 °C and pH 6.5 the peak split into two sharp components at 6.82 and 6.88 ppm, connected by a cross-peak. It was concluded that at 27 °C the side-chain amide resonances of Asn-27 were degenerate.

Two sharp NH resonances were also observed at 7.04 and 7.57 ppm, which showed a strong cross-peak to each other in NOESY spectra. The peak at 7.04 ppm also showed a NOESY cross-peak to the Lys-48 $C^{\alpha}H$ resonance at 4.13 ppm, while the peak at 7.57 ppm showed cross-peaks to both this $C^{\alpha}H$ and a peak at 1.71 ppm that corresponded to one of the Lys-48 $C^{\beta}H$ resonances. These NH peaks could arise from Lys $N^{\zeta}H_3^+$ protons, but their appearance was more consistent with that of a pair of amide NH protons. This raises the possibility that one of the side-chain carboxylates or, more likely, the C-terminus was amidated in our sample of Sh I.

Assignment of Backbone NH Resonances. The complete identification of amino acid spin systems must include the identification of the backbone NH resonances. For this purpose the DQ experiments proved most useful, since 43 out of the 45 expected NH–$C^{\alpha}H$ cross-peaks were observed (Figure 5). A DQF-COSY was used to provide more precise estimates of the $C^{\alpha}H$ chemical shifts and to help analyze overlapping peaks in the DQ spectrum. Using information from RELAY and HOHAHA experiments in H_2O, as well as $C^{\alpha}H$–(NH+$C^{\beta}H$) remote peaks from the DQ spectrum, connectivities to two or more nonlabile side-chain protons could be found for 37 of the expected 45 NH protons. A further

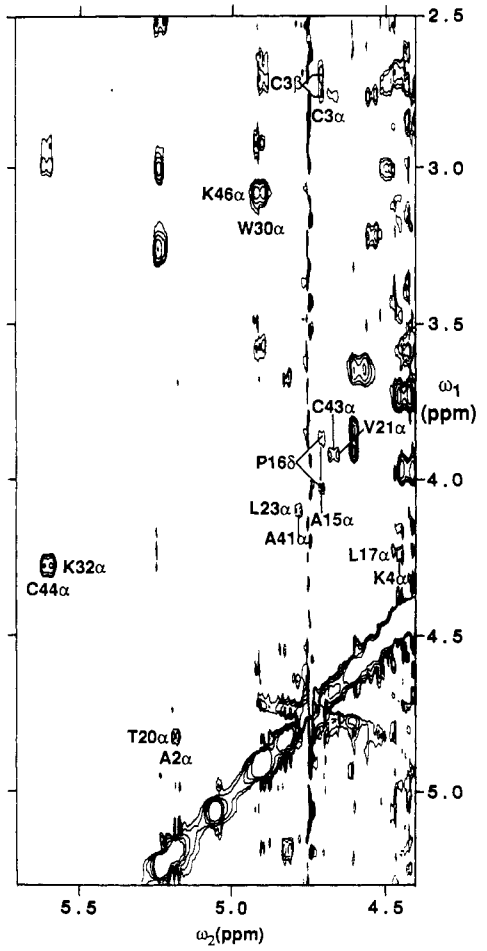

FIGURE 4: $C^{\alpha}H$–$C^{\alpha}H$ region of NOESY spectrum of Sh I in D_2O at pH 5.0 and 27 °C, recorded with 120-ms mixing time. Cross-peaks are marked if they are used in the assignment and are most readily observable in this NOESY experiment. Each cross-peak is designated by the relevant resonance in the ω_1 dimension followed by the corresponding resonance in the ω_2 dimension, e.g., T20α–A2α is the cross-peak at the ω_1 frequency of Thr-20 $C^{\alpha}H$ and the ω_2 frequency of Ala-2 $C^{\alpha}H$.

seven NH protons showed connectivities only to their $C^{\alpha}H$ protons. For Tyr-37, only one NH–$C^{\beta}H$ cross-peak could be found in any of the spectra. Of the 45 NH resonances, 40 could be linked unambiguously to their side chains by matching the chemical shifts of the connected nonlabile proton resonances without relying on chemical shift differences smaller than 0.1 ppm. The $C^{\alpha}H$ resonances of Asp-6, Thr-14, and Thr-38 have identical chemical shifts, as have the $C^{\beta}H$ resonances of these two threonines. The NH resonance of Asp-6 was identified from its sequential NOE connectivities, while the connection between the NH and $C^{\gamma}H_3$ resonances of the threonines was established from intraresidue NOESY cross-peaks and a $d_{\gamma N}(38,39)$ connectivity. Finally, for Cys-3 and Cys-26, the $C^{\alpha}H$ resonance frequencies were very close to both each other and the solvent resonance, and two of the $C^{\beta}H$ resonances overlapped, making it very difficult to distinguish the spin systems. The sequential assignment of the NH resonances was based on ample evidence (Figure 6), but the present assignment of nonlabile proton resonances rests solely on a $d_{\beta N}(3,4)$ sequential connectivity. The relevant Cys-3 $C^{\beta}H$, however, resonates at the same frequency as a Cys-43 $C^{\beta}H$. Considering the presumed existence of a Cys-3–Cys-43 disulfide bond by analogy with the homologous sea anemone toxins ATX I (Widmer et al., 1988) and ATX II (Wunderer, 1978), the cross-peak assigned to $d_{\beta N}(3,4)$ could also arise from a Lys-4 NH–Cys-43 $C^{\beta}H$ long-range connectivity. The present assignment must therefore be regarded as tentative.

Sequential Assignments. Assignment of spin systems to specific residues was carried out by using the sequential NOE connectivities $d_{\alpha N}$, d_{NN}, and $d_{\beta N}$ (Billeter et al., 1982; Wüthrich, 1986), as well as similar distances for prolines involving $C^{\delta}H$ instead of NH (Arseniev et al., 1984). These data were derived primarily from a NOESY spectrum acquired in H_2O at pH 5.0 with a mixing time of 230 ms (Figure 7). NOESY spectra recorded at a different temperature (12 °C) or pH (6.5) were used to help solve assignment problems caused by peak overlap under the original conditions. During the assignment process all AMX spin systems were treated equally, with assignments to individual amino acid types being used only for supporting evidence. As mentioned above, some of the long-chain spin systems were also not differentiated prior to the sequential assignment step.

The observed connectivities on which the sequential assignments are based are summarized in Figure 6, and an example of the procedure followed is shown in Figure 7. The sequential connectivities to the $C^{\delta}H$ resonances of both prolines are typical of prolines preceded by trans peptide bonds (Arseniev et al., 1984). The $d_{\alpha\delta}$ (Ala-15, Pro-16) cross-peaks were too close to the solvent resonance frequency to be observed in H_2O solution but were both observed in a NOESY spectrum recorded in D_2O (Figure 4). Similarly, a number of $d_{\alpha N}$ cross-peaks were bleached out by solvent irradiation at 27 °C but could be distinguished at 12 °C where the solvent resonance was shifted to lower field. Of the five $d_{\alpha N}$ connectivities that remain unobserved, three, viz., $d_{\alpha N}(20,21)$, $d_{\alpha N}(26,27)$, and $d_{\alpha N}(34,35)$, involve $C^{\alpha}H$ resonances that were too close to the solvent resonance at both 12 and 27 °C. A further connectivity, $d_{\alpha N}(6,7)$, was hidden by overlapping peaks in all of the NOESY spectra acquired. Given the large number of sequential connectivities observed, the assignment procedure was relatively straightforward and need not be discussed in further detail.

Under the present conditions, the ^1H NMR spectrum of Sh I contains 265 potentially observable resonances. Methyl groups and the NH_3^+ groups of the lysine side chains and the amino terminus were each counted as one resonance, as were C(2,6)H and C(3,5)H of tyrosines, while the two protons of a methylene group were counted as separate resonances. The $N^{\eta}H_2$ resonances of the two arginines were not included. Of these 265 resonances, 248 have been specifically assigned, corresponding to 94% of the total.

Secondary Structure Elements. The sequential NOE connectivities (Figure 6) show no patterns consistent with helical structures (Billeter et al., 1982; Wüthrich, 1986). Strands 1–6, 18–24, 29–33, and 40–46 show patterns of sequential connectivities and slowly exchanging backbone NH protons consistent with a β-sheet type structure (Wüthrich, 1986). This is confirmed by interstrand NOEs, notably $C^{\alpha}H$–$C^{\alpha}H$ connectivities (Figure 4) that are diagnostic of antiparallel β-sheet. The region of regular secondary structure and the NOEs defining it are shown in Figure 8. The data are compatible with the existence of a four-stranded antiparallel β-sheet extending over residues 1–5, 16–24, 30–33, and 40–46. The location of the β-sheet hydrogen bonds involving residues 1–5 was inferred from the slow exchange rates of the backbone NH protons of Cys-3, Cys-5, Gly-19, and Val-21, as well as the NOE connectivities $d_{\alpha\alpha}(2,20)$, $d_{NN}(3,19)$, $d_{\alpha\alpha}(4,17)$, and $d_{N\alpha}(5,17)$. The sheet can extend no further than the hydrogen bonds shown explicitly in Figure 8. In fact, the limits of the sheet are fairly well-defined by marked deviations from β-sheet like NOE connectivities at residues 16,

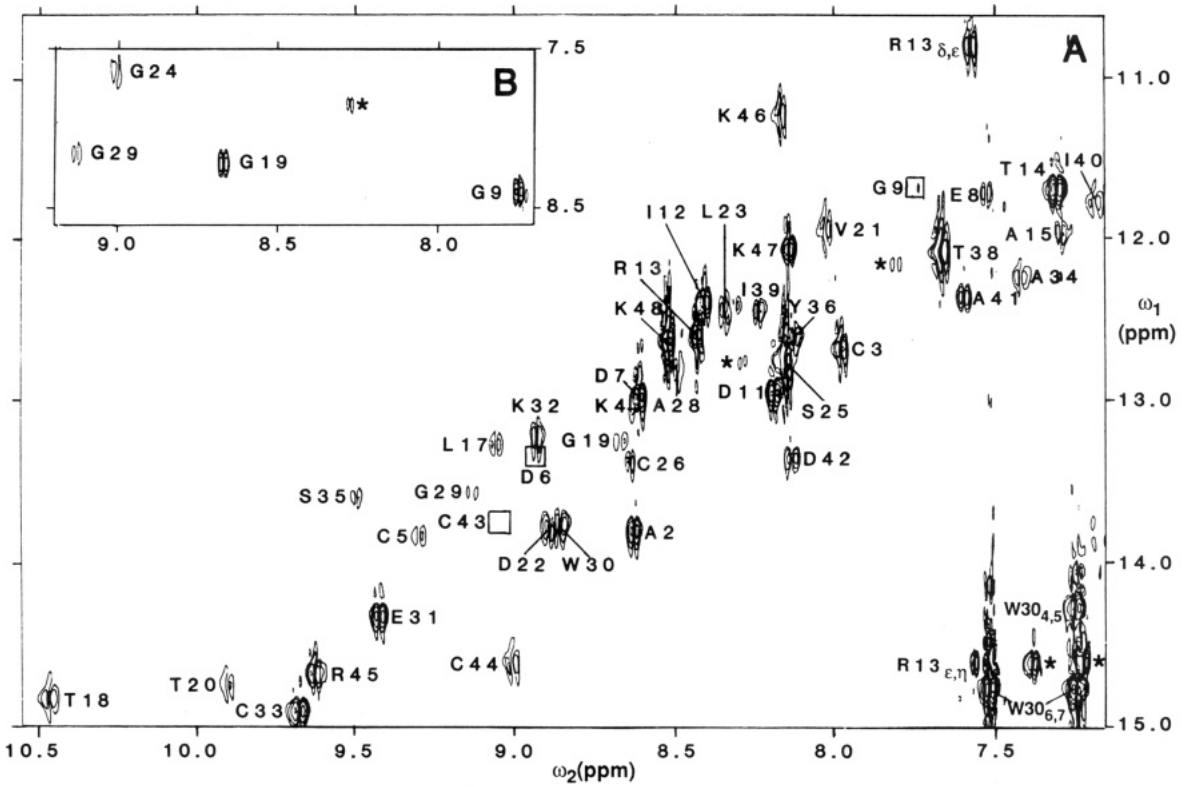

FIGURE 5: DQ spectrum of Sh I in H_2O with 50-ms preparation time. (A) NH–C$^{\alpha}$H region. All peaks are direct rather than remote cross-peaks. The NH–C$^{\alpha}$H peaks of Asp-6 and Cys-43 can be seen at lower plotting levels, as can some glycine NH–C$^{\alpha}$H peaks. (B) NH–(C$^{\alpha}$H+C$^{\alpha}$H) remote peaks of the four glycines in Sh I. Peaks marked by an asterisk (*) are from impurities.

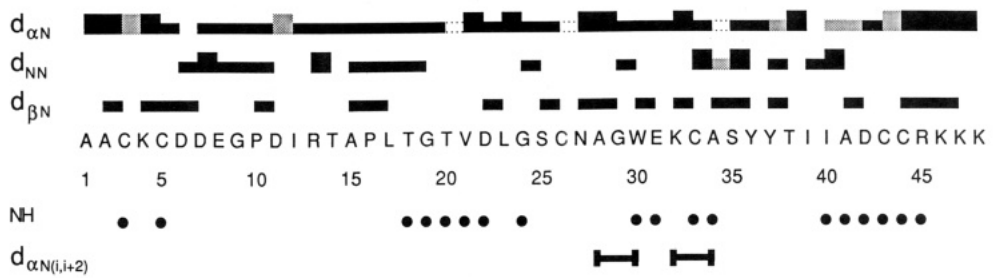

FIGURE 6: Summary of NMR data used for sequence specific assignments and for identification of structural elements of Sh I. Filled bars indicate sequential connectivities observed in a 230-ms mixing time NOESY of Sh I in H_2O at pH 5.0 and 27 °C. Identical notation is used for connectivities involving Pro C$^{\delta}$H, some of which were observed only in a NOESY experiment recorded in D_2O with 120-ms mixing time. Crosshatched bars designate connectivities that were observed only in a 180-ms mixing time NOESY in H_2O at pH 4.9 and 12 °C. $d_{\alpha N}$ connectivities that were masked by the solvent irradiation at both 12 and 27 °C are shown as open, dotted bars. For $d_{\alpha N}$ and d_{NN} connectivities, thick and thin bars represent strong and weak cross-peaks, respectively, relative to an arbitrary reference level. Slowly exchanging backbone NH protons as defined in the preceding paper (Norton et al., 1989) are indicated by filled circles in the NH column. The NH of Thr-18 exchanges significantly faster than the other slowly exchanging amides indicated (Norton et al., 1989).

25, 29, 34, and 40, and by the N- and C-termini.

A significant distortion of the β-sheet structure must be present in the region of residues 17 and 18. This is shown by the strong $d_{NN}(17,18)$ and $d_{NN}(18,19)$ connectivities, which are not expected in an extended structure, and the presence of a strong $d_{\alpha\alpha}(4,17)$ interstrand connectivity instead of the $d_{\alpha\alpha}(4,18)$ connectivity expected of a regular antiparallel sheet. In addition, no strong $d_{\alpha\alpha}$ NOEs were observed between either of the Gly-19 C$^{\alpha}$Hs and Arg-45 C$^{\alpha}$H, where at least one would be expected. Finally, whereas the amide exchange rates of Thr-18 and Lys-46 should be similar to those of other hydrogen-bonded amides in a regular sheet, the observed exchange rate of Thr-18 was much faster than those of nearby residues such as Cys-3 and Gly-19, and that of Lys-46 was too fast to measure under comparable conditions (Norton et al., 1989). The distortion indicated by these observations appears to correspond to one of the various types of β-bulge identified by Richardson et al. (1978).

The absence of several NOESY cross-peaks expected in the proposed secondary structure could in each case be rationalized by peak overlap or by the effect of the solvent presaturation. NOE cross-peaks involving the C$^{\alpha}$H resonances of Lys-4 and Leu-17 could not be unambiguously assigned, because other C$^{\alpha}$H protons resonate at the same chemical shift. The assignment of these NOEs to these residues was justified, however, by NOEs observed between one Leu-17 C$^{\delta}$H$_3$ and each of Lys-4 NH, Cys-5 NH, Leu-17 NH, Thr-18 NH, and the C$^{\alpha}$H resonances assigned as Lys-4 C$^{\alpha}$H and Leu-17 C$^{\alpha}$H. Likewise, the C$^{\alpha}$H resonances of Leu-23 and Ala-41 have the same chemical shift as other C$^{\alpha}$H resonances. In this case the present assignment of NOEs was justified by a series of NOE cross-peaks observed between Ala-41 C$^{\beta}$H$_3$ and each of Gly-24 NH, Asp-42 NH, and the C$^{\alpha}$H of either Leu-23 or Ser-35.

The cross-peaks connecting Ala-28 C$^{\alpha}$H to Trp-30 NH and Lys-32 C$^{\alpha}$H to Ala-34 NH are indicative of turns involving residues 27–30 and 33–34, respectively. The pattern of se-

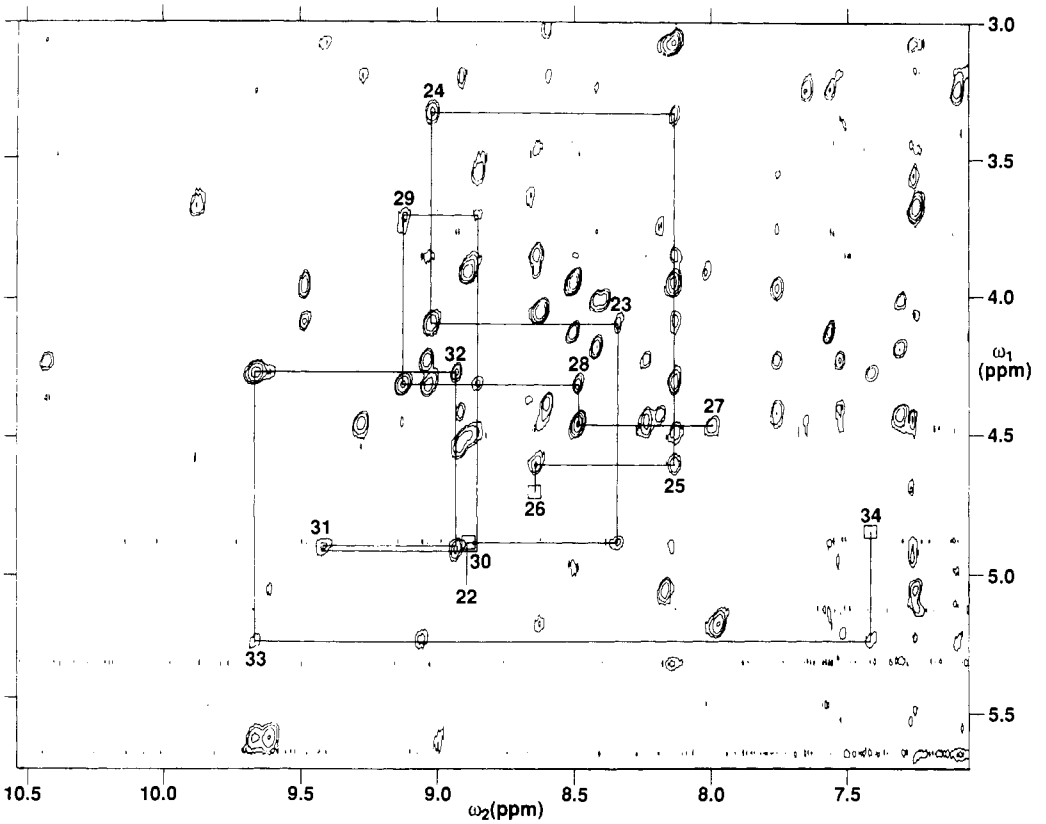

FIGURE 7: Fingerprint region of a NOESY spectrum of Sh I in H_2O at pH 5.0 and 27 °C recorded with 230-ms mixing time. The spectrum was recorded without sample spinning in an attempt to minimize t_1 noise. The series of cross-peaks used to assign residues 22–26 and 27–34 is shown. The intraresidue NH–C$^\alpha$H cross-peaks are marked with the residue number and are shown as empty squares if unobserved.

quential NOEs and slowly exchanging NHs expected for a type II β-turn or half-turn involving residues i to $i + 3$ is an observable $d_{\alpha N}(i+1,i+3)$, strong $d_{\alpha N}(i+1,i+2)$ and $d_{NN}(i+2,i+3)$, and weak $d_{\alpha N}(i+2,i+3)$ and $d_{NN}(i+1,i+2)$, together with a slowly exchanging $i + 3$ NH proton (Wüthrich, 1986). This pattern, which is clearly different from the one characteristic of types I, I′, or II′ reverse turns, was seen for both residues 27–30 and 31–34. It is highly probable that Sh I does indeed contain a type II β-turn involving residues 27–30, considering the facts that residue 29 is a glycine, as is most often observed in position $i + 2$ of type II β-turns, and that the secondary structure must incorporate some kind of turn around this position in order to accommodate residues Ser-25 and Trp-30 at opposite ends of the β-sheet-like structure. In contrast, the involvement of residues 31–33 in the β-sheet and the presence of a cysteine rather than a glycine at position 33 makes it very unlikely that residues 31–34 are involved in a regular type II β-turn or half-turn. Since tight turns are difficult to identify solely on the basis of data such as these (Wüthrich, 1986), final conclusions on these secondary structure elements are best deferred until the tertiary structure has been determined.

Discussion

In this paper an essentially complete set of sequence-specific resonance assignments has been described for Sh I. The strategy followed in making these assignments was similar to the sequential assignment procedure outlined by Wüthrich and co-workers (Wüthrich, 1986). The use of HOHAHA experiments greatly facilitated the assignment of long-chain spin systems and proved useful in linking backbone amide resonances to those from C$^\alpha$H and C$^\beta$H of the same side chain.

Nearly complete sets of ^{1}H NMR assignments at 500 MHz are now available for two stichodactylid polypeptides, Sh I and Hp II (Wemmer et al., 1986), and two actiniid polypeptides ATX I (Widmer et al., 1988) and AP-A (B. C. Mabbutt and R. S. Norton, unpublished results). While comparisons among these data sets are complicated by differences in conditions of pH and temperature, some inferences can be drawn. The ranges of NH and C$^\alpha$H chemical shifts across this series of four polypeptides[2] are shown in Figure 9. There are eight spin systems in which both the NH and C$^\alpha$H chemical shifts have a range $\leq|0.3|$ ppm, viz., Cys-3, Asp/Ser-7, Gly-9, Arg-13, Pro/Thr/Ser-16, Thr-20[2], Gly-29, and Arg/Lys-45. For Cys-5, the NH and C$^\alpha$H ranges are 0.31 and 0.19, respectively, while for Pro-10 the C$^\alpha$H range is only 0.05 ppm. It is interesting to note that only three of these residues, viz., Cys-3, Thr-20, and Arg-45, occur within the β-sheet region, while Cys-5 occurs at the edge of the sheet. The remaining six represent residues that have similar magnetic environments in all four molecules. Considering the extent of homology among the four polypeptides, it is likely that these residues also occur within similar structural features. In the case of Gly-29 this common structural feature is a reverse turn, as described above. Clearly this type of comparison does not detect all amino acid residues that participate in structures common to the four polypeptides, partly because the aromatic residues, which have a significant effect on chemical shifts from surrounding residues (Wüthrich, 1986), are not conserved throughout the series. It does, however, highlight some that would not have been inferred from inspection of the ordered

[2] In comparing the chemical shifts of Sh I with those of Hp II (Wemmer et al., 1986), it was noted that the value reported for Thr-20 NH in Table II of Wemmer et al. was 7.76 ppm. On the basis of data presented in Figure 3 of their paper and by analogy with Sh I, AP-A (B. C. Mabbutt and R. S. Norton, unpublished results), and ATX I (Widmer et al., 1988), it appears that this chemical shift should read 9.76 ppm.

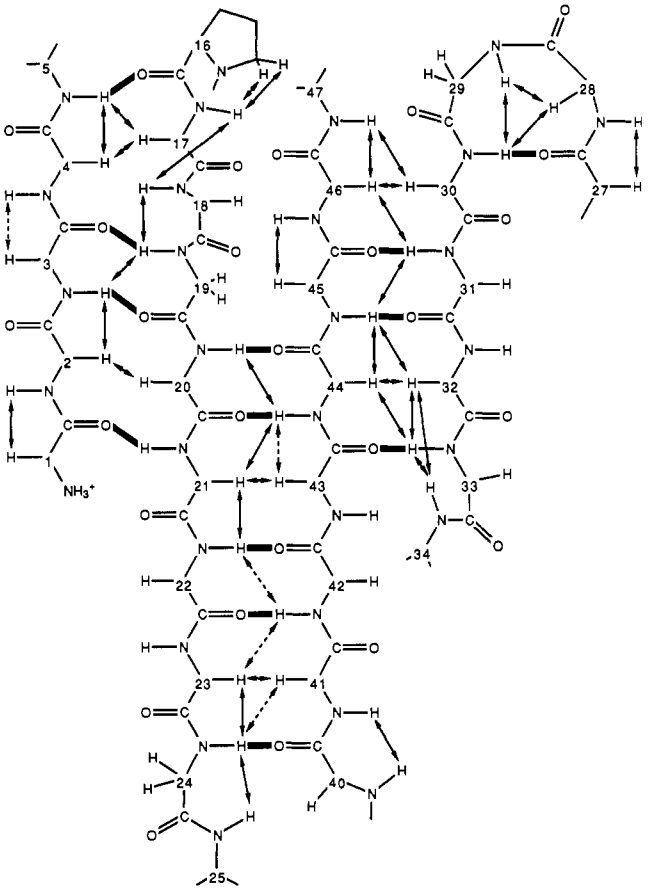

FIGURE 8: Secondary structure elements in Sh I as determined by ^{1}H NMR in aqueous solution at pH 5.0 and 27 °C. The secondary structure comprises a tight turn at residues 27–30 and an antiparallel β-sheet involving residues 1–5, 16–24, 30–33, and 40–46. Evidence for this structure comes from strong $d_{\alpha N}$ connectivities (Figure 6), from slowly exchanging backbone NHs (Figure 6), and from other observed NOE connectivities as shown. Probable hydrogen bonds (shown by thick lines) are indicated for those NH protons that exchange slowly with solvent (Norton et al., 1989). These hydrogen bonds define the largest possible extent of β-sheet-like structure. NOEs observed are drawn as arrows if they are observable at 27 °C with a 230-ms mixing time and as broken arrows if they are observable only at 12 °C with a 180-ms mixing time. Weak $d_{\alpha N}$ connectivities (see Figure 6) are not shown.

secondary structure and the disulfide bonds.

The ordered secondary structure in Sh I has been defined from the nature and location of both sequential and interstrand NOEs, as well as peptide NH exchange rates. Our data are consistent with a four-stranded antiparallel β-sheet involving residues 1–5, 16–24, 30–33, and 40–46, with a β-bulge at residues 17 and 18. A tight turn, probably a type II β-turn, has been identified at residues 27–30. A less well-defined turn is also present at residues 33–34.

Secondary structure elements similar to those in Sh I have been identified from ^{1}H NMR studies of the related polypeptides AP-A (Gooley & Norton, 1986), ATX I (Gooley & Norton, 1986; Widmer et al., 1988), and Hp II (Wemmer et al., 1986). The presence of a β-bulge at residues 17 and 18 was noted in ATX I by Widmer et al. (1988), although not in AP-A or Hp II. However, in a more complete set of sequential resonance assignments for AP-A obtained recently (B. C. Mabbutt and R. S. Norton, unpublished results), NOE connectivities compatible with the presence of such a β-bulge are observed. Although the cysteine pairing in the three disulfide bonds of Sh I has not been determined chemically, it is reasonable to assume that it will be the same as that determined for the related polypeptide ATX II (Wunderer,

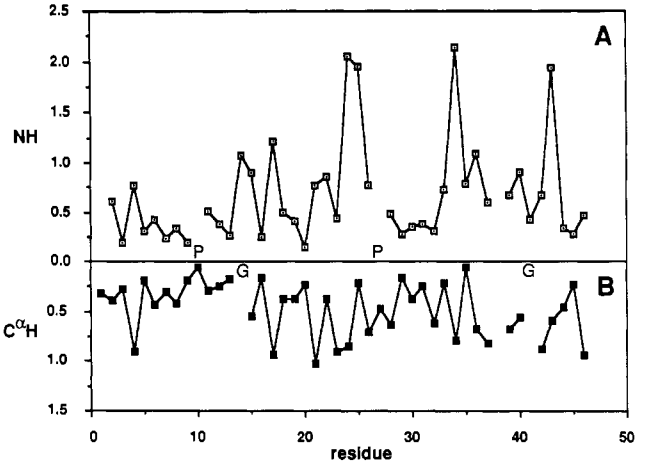

FIGURE 9: Range of chemical shifts (in ppm) of NH (A) and $C^\alpha H$ (B) resonances across the four polypeptides Sh I, Hp II, ATX I, and AP-A, with sequences aligned as in Figure 1 and numbered according to Sh I. P at positions 10 and 27 indicates that no comparison of NH chemical shifts was made because of the presence of two or more proline residues. At positions where only one proline was present the range of NH chemical shifts covers the remaining three residues, while that for $C^\alpha H$ includes all four. G at positions 14 and 41 indicates that no comparison of $C^\alpha H$ chemical shifts was made because of the presence of two nonconserved glycine residues. Where only one nonconserved glycine was present (at positions 24, 25, 35, and 37), its $C^\alpha H$ chemical shifts were omitted from the calculated range; in all cases inclusion of both Gly $C^\alpha H$ chemical shifts would have extended the range shown in this Figure. No values are shown for position 38 as this residue is deleted in ATX I and its chemical shifts in AP-A were not reported. Comparisons were also omitted for the additional N-terminal residue in ATX I and AP-A, the two additional C-terminal lysines in Sh I and Hp II, and the two additional nonconserved residues in AP-A at positions 26 and 27 (see Figure 1).

1978). This should be confirmed during the tertiary structure determination (R. H. Fogh, W. R. Kem, and R. S. Norton, unpublished results). In any case, it is clear that the β-sheet must be distorted in order to accommodate these disulfide bonds. This distortion would be facilitated by the presence of a β-bulge.

As noted under Materials and Methods, HPLC analysis of the sample of Sh-I used in these studies revealed the presence of minor polypeptide impurities comprising up to 10–15% of the material. These impurities did not interfere with the assignment of resonances from the major component, although impurity peaks were clearly evident in the 2D spectra. Because of the presence of these impurity peaks, however, we cannot exclude the possibility that some resonances of Sh I undergo splitting due to the presence of a minor conformer in solution. It can be excluded that Sh I displays major conformational heterogeneity of the type observed in AP-A and ATX II (Gooley et al., 1984, 1988). In this respect, Sh I is similar to ATX I (Widmer et al., 1988; Gooley et al., 1988).

The biological effects of Sh I, Hp II, AP-A, and ATX I collectively span a wide range with respect to species specificity, tissue specificity, and potency. Furthermore, as outlined in the introduction, there are significant differences between the stichodactylid class of polypeptides, represented by Sh I and Hp II, and the actiniid class, represented by AP-A and ATX I. Clear differences are also observed between the ionization behavior and thermal stability of Sh I and those of AP-A and ATX I, as described in the preceding paper (Norton et al., 1989). At the level of the secondary structure elements identified from NMR data, however, all four polypeptides are strikingly similar. It is apparent that determination of the complete tertiary structures of these polypeptides by means of distance geometry and restrained molecular dynamics

calculations based on NMR data will be required before the structural basis of the different biological activities of these polypeptides can be accounted for.

Registry No. Sh I, 117860-13-6.

REFERENCES

Arseniev, A. S., Kondakov, V. I., Maiorov, V. N., & Bystrov, V. F. (1984) *FEBS Lett. 165*, 57–62.

Bax, A., & Davis, D. G. (1985) *J. Magn. Reson. 65*, 355–360.

Bax, A., & Drobny, G. (1985) *J. Magn. Reson. 61*, 306–320.

Beress, L. (1982) *Pure Appl. Chem. 54*, 1981–1994.

Billeter, M., Braun, W., & Wüthrich, K. (1982) *J. Mol. Biol. 155*, 321–346.

Braunschweiler, L., & Ernst, R. R. (1983) *J. Magn. Reson. 53*, 521–528.

Braunschweiler, L., Bodenhausen, G., & Ernst, R. R. (1983) *Mol. Phys. 48*, 535–560.

Dunn, D. (1981) *Trans. Am. Philos. Soc. 71*, 3–115.

Gooley, P. R., & Norton, R. S. (1986) *Biochemistry 25*, 2349–2356.

Gooley, P. R., Blunt, J. W., & Norton, R. S. (1984) *FEBS Lett. 174*, 15–19.

Gooley, P. R., Blunt, J. W., Beress, L., & Norton, R. S. (1988) *Biopolymers 27*, 1143–1157.

Jeener, J., Meier, B. H., Bachmann, P., & Ernst, R. R. (1979) *J. Chem. Phys. 71*, 4546–4553.

Kem, W. R. (1988) in *The Biology of Nematocysts* (Hessinger, D., & Lenhoff, H., Eds.) pp 375–405, Academic Press, New York.

Kem, W. R., Dunn, B. M., Parten, B. F., Pennington, M. W., & Price, D. (1986) *Fed. Proc., Fed. Am. Soc. Exp. Biol. 45*, 1795.

Levitt, M. H., & Freeman, R. (1979) *J. Magn. Reson. 33*, 473–476.

Macura, S., Huang, Y., Suter, D., & Ernst, R. R. (1981) *J. Magn. Reson. 43*, 259–281.

Marion, D., & Wüthrich, K. (1983) *Biochem. Biophys. Res. Commun. 113*, 967–974.

Metrione, R. M., Schweitz, H., & Walsh, K. A. (1987) *FEBS Lett. 218*, 59–62.

Müller, N., Ernst, R. R., & Wüthrich, K. (1986) *J. Am. Chem. Soc. 108*, 6482–6492.

Norton, R. S., Cossins, A. I., & Kem, W. R. (1989) *Biochemistry* (preceding paper in this issue).

Norton, T. R. (1981) *Fed. Proc., Fed. Am. Soc. Exp. Biol. 40*, 21–25.

Piantini, U., Sørensen, O. W., & Ernst, R. R. (1982) *J. Am. Chem. Soc. 104*, 6800–6801.

Richardson, J. S., Getzoff, E. D., & Richardson, D. C. (1978) *Proc. Natl. Acad. Sci. U.S.A. 75*, 2574–2578.

Schweitz, H., Bidard, J.-N., Frelin, C., Pauron, D., Vijverberg, H. P. M., Mahasneh, D. M., Lazdunski, M., Vilbois, F., & Tsugita, M. (1985) *Biochemistry 24*, 3554–3561.

Shaka, A. J., & Freeman, R. (1983) *J. Magn. Reson. 51*, 169–173.

Torda, A. E., Mabbutt, B. C., van Gunsteren, W. F., & Norton, R. S. (1988) *FEBS Lett.* (in press).

Wagner, G. (1983) *J. Magn. Reson. 55*, 151–156.

Wagner, G., & Zuiderweg, E. R. P. (1983) *Biochem. Biophys. Res. Commun. 113*, 854–860.

Wemmer, D. E., Kumar, N. V., Metrione, R. M., Lazdunski, M., Drobny, G. & Kallenbach, N. R. (1986) *Biochemistry 25*, 6842–6849.

Widmer, H., Wagner, G., Schweitz, H., Lazdunski, M., & Wüthrich, K. (1988) *Eur. J. Biochem. 171*, 177–192.

Wokaun, A., & Ernst, R. R. (1977) *Chem. Phys. Lett. 52*, 407–412.

Wunderer, G. (1978) *Hoppe-Seyler's Z. Physiol. Chem. 359*, 1193–1201.

Wüthrich, K. (1986) *NMR of Proteins and Nucleic Acids*, Wiley, New York.

Zykova, T. A., Vinokurov, L. M., Kozlovskaya, E. P., & Elyakov, G. B. (1985) *Bioorg. Khim. 11*, 302–310.